J. Univ. Kuwait (Sci.) **21**, 1994

Three dimensional non-linear cracking analysis of prestressed concrete containment vessel

Y.F. AL-OBAID

Faculty of Technological Studies, PAAET P.O. Box 42325, Shuwaikh 70654 Kuwait

ABSTRACT

The paper gives full development of three-dimensional cracking matrices. These matrices are simulated in three-dimensional non-linear finite element analysis adopted for concrete containment vessels. The analysis includes a combination of conventional steel, the steel line r and prestressing tendons and the anisotropic stress-relations for concrete and concrete aggregate interlocking. The analysis is then extended and is linked to cracking analysis within the global finite element program **OBAID**. The analytical results compare well with those available from a model test.

INTRODUCTION

In nuclear plant design, components, equipment and structure should be protected (Al-Obaid 1984, 1986, 1992) against hazards such as cracks in concrete vessel. The representation of cracks in concrete is a complex phenomenon, particularly in the context of concrete pressure vessels. This paper attempts to give a step by step analysis of initiation, closure and re-opening of cracks under overload conditions. The influence of creep and concrete aggregate interlocking has been examined and is included in the overall analysis.

The three-dimensional elements which have been used in this analysis are the isoparametric, panel and line elements (Fig. 1) representing concrete, the line r, the prestressing tendons and bonded reinforcement of the vessels. Appendix I indicates the procedures of computing stiffness matrices, stresses, strains and load-displacement relations for these elements. The volume integrals given in this appendix are solved using numerical integration and Gaus quadrature. By using strain-displacement relations and particular constitutive laws, the stresses and strains are evaluated in terms of nodal displacements. The strain energy of the entire vessel already discretized is then obtained by adding the contributions to all of its elements. Using the principle of minimum potential energy, linear equations are initially produced relating the generalized nodal displacements and generalized externally applied loads in the form given by

$$[K]\{U\} = \{F\} \tag{1}$$

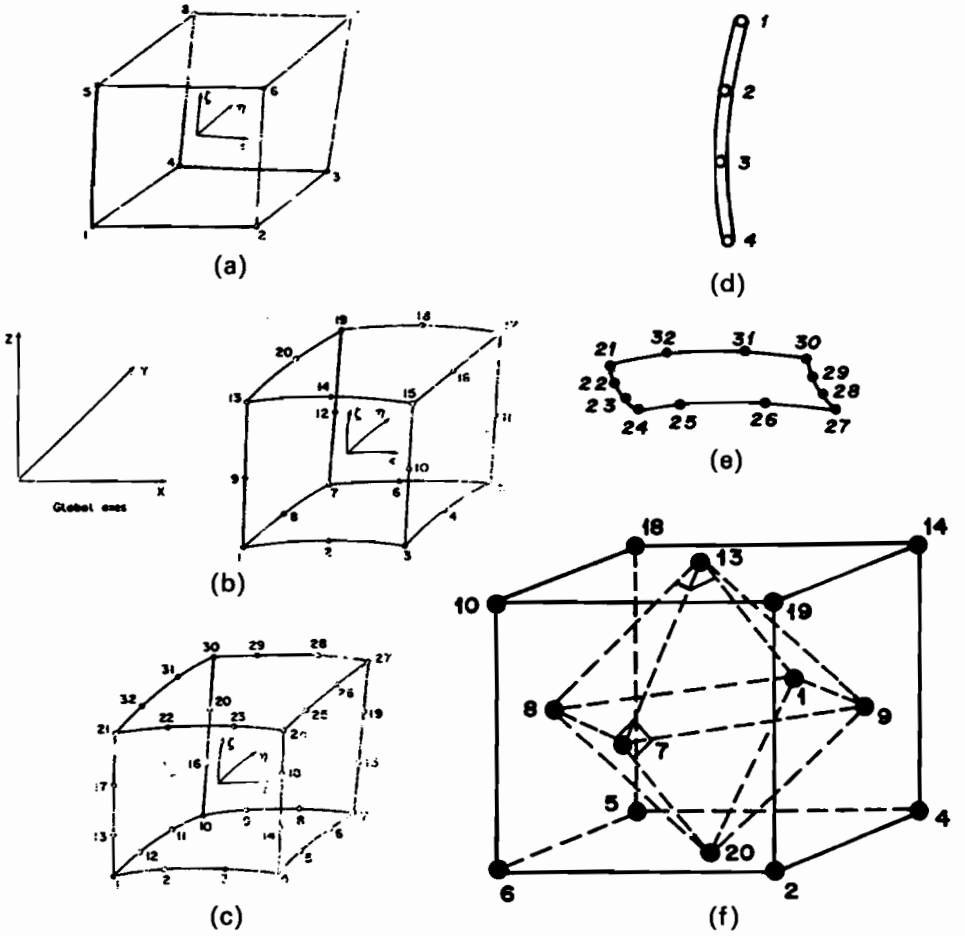

Fig. 1. Isoparametric elements. (a) Eight-noded solid element; (b) twenty-noded solid element; (c) thirty-two-noded solid element; (d) four-noded Bar element; (e) twelve-noded Linar element; (f) typical location of integration points for 20 noded element.

where $[K]$ is the overall stiffness matrix, $\{U\}$ is the generalized displacements and $\{F\}$ is the nodal loads caused by internal and external pressures or loads on a vessel. Appendix I gives the entire formulation including the effect of three-dimensional creep.

The paper then proceeds to establish a criterion for a three-dimensional cracking of vessels. It is followed by a step-by-step analysis for computing incremental stresses, total stresses and strains and a check on the initiation of cracks and their directions using a standard transformation. Stresses are converted into nodal loads and the residual forces are examined and checked at the end of each iteration and finally the iteration terminates.

The Computer program **OBAID** has the options for the solution of equations using BLOCKING TECHNIQUE and DIRECT ELIMINATION. The convergence of the iterative solution is closely related to a uniform acceleration. The vessel elements are simultaneously examined for concrete crushing, and yielding of steel. Provision is

made for closure and opening of cracks. Appendices I and II give concrete constitutive laws, representing the anisotropic behavior of concrete and the three-dimensional cracking matrices developed on the basis of the argument given in this paper. Prototype vessels and a model cap of a vessel have been examined. The analytical results obtained are plotted along with the model test and data available from elsewhere. These result are in good agreement with each other.

THREE-DIMENSIONAL CRACKING OF VESSELS

Several tests have been conducted and they indicate progressive rather than sudden explosive failure. Under incremental loads, progressive and well disposed cracks occur. In the light of these experiments, the following assumptions are made for the initiation and closure and re-opening of cracks at Gaussian integration points of the finite element model:

(a) Where cracks occur the direct tensile stress cannot be supported in the direction normal to the cracks.
(b) A concrete element parallel to the crack is assumed to carry a stress given by the constitutive relationship consistent with biaxial or triaxial conditions prevailing in the plane parallel to the crack. On further loading new cracks occur at some angle to the previous ones.
(c) The opposite faces to a crack opening in a normal direction will interlock when they are subjected to a parallel differential movement. As a result, restraining of movement and volume changes will cause forces which will only be transmitted across the crack. With large crack widths, these surfaces would completely separate and the aggregate interlock phenomenon would cease. If the strain across the crack is positive, the crack is considered open and rigidity for that direction is kept zero.
(d) Where interlocking exists, the shear stress to τ_0 along the crack will not be zero and instead it is linearly related to the strain caused by the differential movement.
(e) During the unloading procedure of the vessel, the differential movement between faces of a crack and the surface deterioration will not interfere with the closing of a crack. A crack closes if the normal (negative quantity) across the crack is compressive.

The best way to handle these cracks is to adjust material laws in zones where they occur with their natural directions. The material matrices $[D]$ given in Appendix I can easily be modified to initiate cracks in specific directions using direction cosines.

STEPS FOR CRACK ANALYSIS

The cracks are initiated, closed and re-opened using the following steps:–

1. Enter in subroutine CRACK of program OBAID initial strains

   $\{E_0\}$

   Initial stress $\{\sigma_{in}\}$ and adjusted material property matrix

   $[D]$.

2. Compute incremental stresses

   $$\delta\{\sigma_i\} = [D]\delta\{\epsilon\}_i \text{ for no crack} \tag{2}$$

or

$\delta\{\sigma_i\}^* = [D]\delta\{\epsilon\}_i$ for already initiated crack

3. Calculate total stresses and strains

$$\{\sigma_i\} = \{\sigma_{in}\}^* + \delta\{\sigma_i\}^* \tag{3}$$

$$\{\epsilon\}_i = \{\epsilon_{in}\} + \delta\{\epsilon\}_i$$

* is excluded if cracks do exist.

4. For initially uncracked condition, compute principal stresses $\{\sigma\}$ corresponding to total stresses in section (3) and check for the initiation of cracking

$$\{\sigma\}_p \geqslant \sigma_i \tag{4}$$

If the above inequality is satisfied, calculate the angle of cracks and their directions. Principal stresses are calculated and converted into global system using a standard transformation matrix $[T'']$

$$\{\sigma_g\} = [T'']\{\sigma\}_p, \tag{5}$$

5. The stresses are converted into nodal loads

$$\{F\} = [B]_g^T\{\sigma\}dvol. \tag{6}$$

6. Residual forces are examined and accumulated for elements and are checked at the end of each iteration. The final iteration terminates when the values of these forces are less than a predetermined constant (0.001).
7. In the meantime it is essential to examine also the crushing of concrete and yielding of steel. When the principal compressive strain is $\epsilon_i \geqslant \epsilon_{cu}$, the limiting compressive strain (assumed 0.0035), concrete crushes in the compressive zones at the Gaussian integration points. The material matrix $[D]^*$ is set to zero. The stresses are then zero and for subsequent load increments these points are ignored. Stresses at these points are converted into equivalent nodal forces as shown in Eqn (6). The steel elements, whether lying within or on the solid element, yield on the basis of uniaxial stress-strain relationship.
8. This criterion for crack closure is based on the inequality of strains (Fig. 2)

$$\epsilon_{cv} \leqslant \epsilon_c \tag{7}$$

where ϵ_{cv} = strain normal to the crack

$\epsilon_c = \dfrac{v^*}{E^*} \cdot \sigma_{cu}$ or strain from the stress-strain curve

E^* & v^* = relevant concrete Young's modulus and Poissons ratio

If $\epsilon_{cv} < \epsilon_c$ compressive strains are induced which may not be compatible with the concrete strains. When cracks are closed at an intermediate load within the increment then at the end of the load increment stresses may occur at the contact faces of the crack.

9. The opening of the crack is similar to new crack initiation. The only difference is the tensile resistance offered by concrete. The closed crack will re-open if

$$\sigma_{cv} \geqslant 0 \tag{8}$$

The shear stresses T_{cv} on the crack interface and the normal stresses σ_{cv} must be

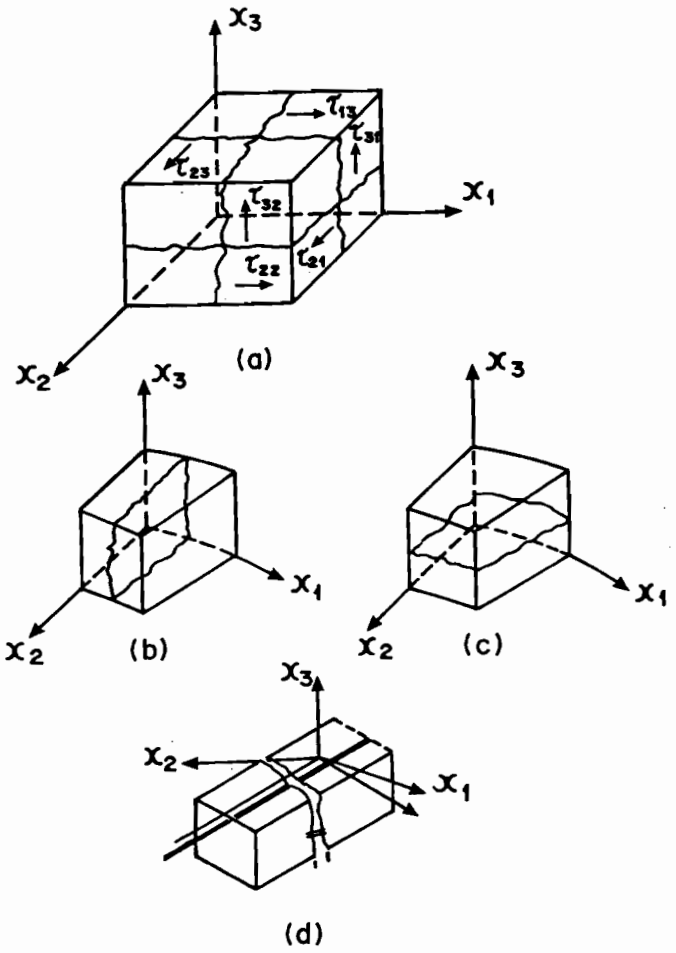

Fig. 2. Typical Crack Propagation. (a) General cracking pattern with shear across and perpendicular to cracks; (b) radial crack; (c) circumferential crack; (d) reinforcement & cracks.

redistributed such that

$$\hat{\imath}_{fv} = \sigma_{cv} \tag{9}$$

$$\hat{\imath}_{f\tau} = \tau_{cv}$$

When these stresses are equated, the rest of the procedure should then be the same as given earlier.

10. The modes of cracking are not identical from one iteration to another at any specific Gaussian point. The most obvious reasons for the improvement in $[D]^*$ and the effect of interlocking with the shear stress along the crack. These changes from one crack node to another are included in the program **OBAID**. The following linear relationship is adopted for shear τ^*

$$\tau^* = a'GY^* \tag{10}$$

where G is the shear modulus of uncracked material
a' is the interlocking factor.

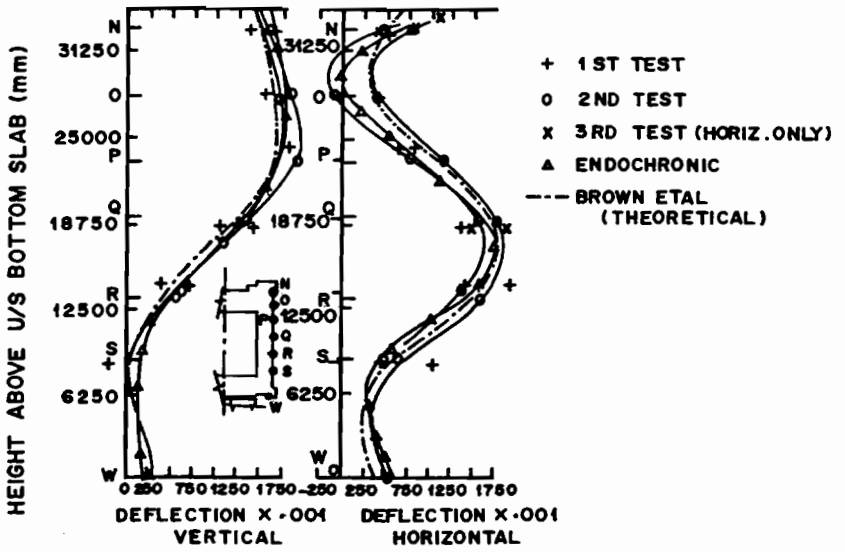

Fig. 3. Wall horizontal and vertical deflection.

APPLICATION TO CASE STUDY

The Oldbury Vessel parameters are chosen. The helical cables of 22 layers (160 cables/layer) are placed clockwise and anti-clockwise. A 45 degree helix forms a barrel shape structure. In the cap the horizontal prestressing consists of 30 cables per layer (total 20 layers) pass through the network of helical cables. The cables are anchored in four galleries. External loads due to these cables are computed and are applied at appropriate levels. A typical *3D 20* noded isoparametric finite element is chosen for

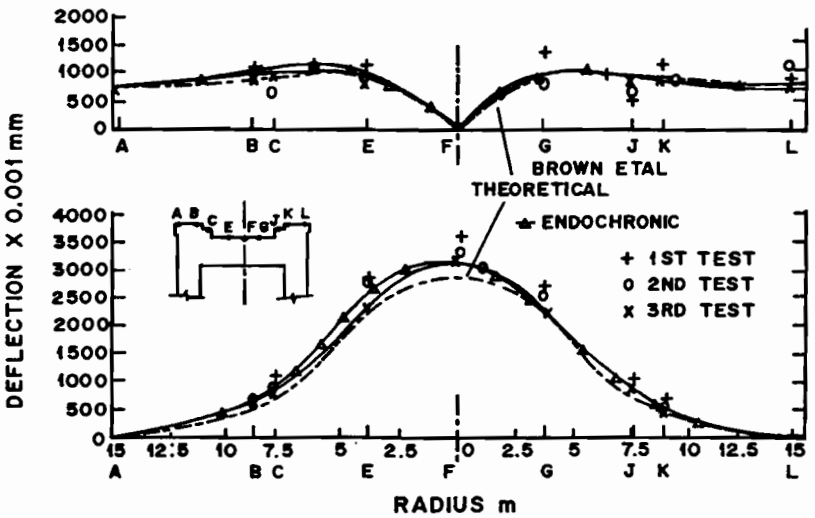

Fig. 4. Top slab horizontal and vertical deflections.

the vessel concrete with $3D$ line and membrane elements for prestressing cables and linear. The effect of linear anchorage is ignored.

The vessel was analyzed for the design pressure, temperature, creep and prestressing loads (operational condition for a period of 7 years).

The analysis is then adjusted to be in line with the test pressures considered by Brown and Bland (1975). Figures 3 and 4 show a comparative study of deflections for the barrel wall and the top cap. For the ultimate loading conditions, in addition to the normal operational loads of the vessels, the pressure in all cavities of the vessel is increased monotonically until failure occurs. The internal pressure to the point of failure of vessel is applied in 12 increments. The first increment is slightly above the normal operational condition loads (prestress forces, internal pressure at the design level and temperature loads) and the rest of the increments are carefully chosen as a fraction of the design pressure. This decision is taken so as not to cause any excessive non-linearity within the load increments. Analyses are performed at the following

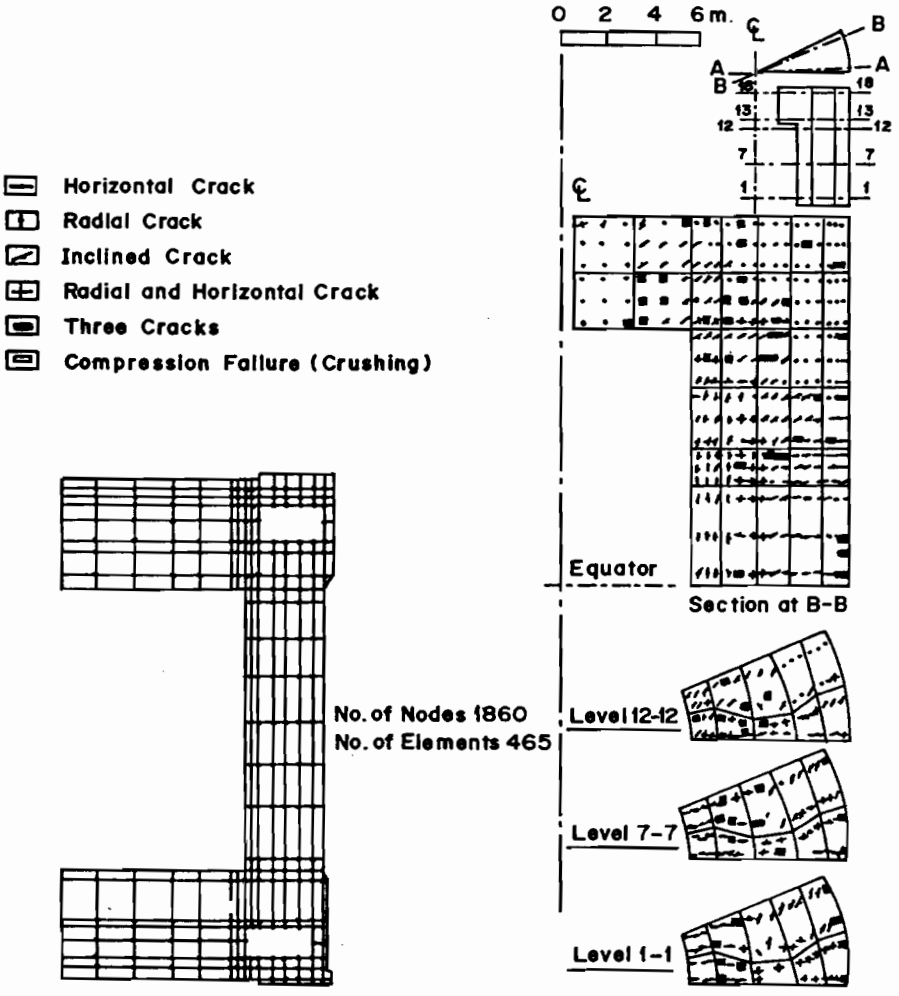

Fig. 5. Crack Pattern of the vessel.

pressures (N/mm^2):

2.66,	3.75,	3.99,	4.665,	4.825,	5.32,
5.985,	6.65,	7.98,	8.645,	9.975,	11.305

The constant stiffness method (initial stress method) is used for all cases analyzed in this section. An average of 10 iterations per increment were required for the convergence of the solution. Iterations within each load increment are terminated when a norm of residuals has reached a specified tolerance of 3×10^{-2}. Figure 5 shows crack pattern of the vessel.

The analysis also take into account the changing material properties with time and have been performed for 10 years, 20 years and 30 years in terms of prestress losses and material properties.

The obtained results of these analysis are not reported, in the form of pressure-deflection curves, stud loads, bifurcation and liner rupture under the crack patterns of the vessels. Using the crack widths obtained previously for the liner yielding and rupturing, the analytical results show that due to the influence of the liner, the load carrying capacity is increased by about 15%. Figure 6 shows the collapse mode given a load factor of 4.25.

REMARKS

1. Due to the limitation and space, it was not possible to give detailed information on fracture criteria. Although the art of non-linear cracking analysis is well developed (Al-Obaid 1992), the science is just beginning to be understood, and theory still represents a controversial field. This is due to the complexity of cracking behaviour in prestressed concrete, which still requires further study and research. Therefore it is hoped in another contribution to highlight the main aspects of the cracking and fracture criteria with a view. To embracing a wide body of related phenomena which will assist in future theoretical and experimental work.

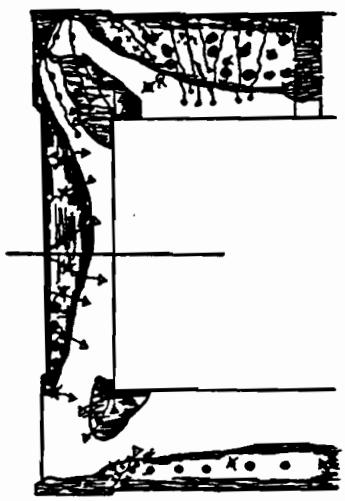

Fig. 6. Collapse mode of OLDBURY prestressed Concrete Reactor Pressure vessel.

2. The three-dimensional cracking of prestressed concrete vessels is conveniently and readily solved by means of this unified method. The combination of several elements and their interactions under overload conditions can provide the solution to many problems. The Direct Elimination Procedure and Blocking Technique proved to be very useful in calculating stresses, strain and cracks. An enormous effort was required to evaluate both sizes and direction of cracks including conditions for closure and re-opening of cracks. This method has been applied on one existing vessels and the results obtained are in good agreement with the available data.

The method presented for cracks can be used for other structures under both static and dynamic loads.

ACKNOWLEDGEMENT

The author extends gratitude to the Simon-Carve Ltd for the availability of data and to Taylor Woodrow Construction Ltd from whom the author obtained first inspiration.

REFERENCES

Al-Obaid, Y.F. 1984. Dynamic crack propagation in **PWR** tube. Pressure Vessel and Piping Conference (ASME), June 17–21, Houston, Texas, U.S.A.

Al-Obaid, Y.F. 1986. The finite element analysis of crack growth in zircaloy tubing under extreme temperature, International Journal of Engineering Fracture Mechanics, **23 (5):** 875–82.

Al-Obaid, Y.F. 1992. Three-dimensional cracking analysis of concrete containment vessels under external impacts. Journal of the University of Kuwait (Science), **19 (1):** 17–34.

Brown, V. & Bland, A. 1975. The operator's view of the first seven years service of the concrete pressure vessels at Oldbury-on-Severn Power Station. International conference of pressure and containment vessels, York, England.

(Received 20 March 1993, revised 20 November 1993)

APPENDIX I

BASIC FORMULATION

1. The displacement field within each element is given by

$$\{U\} = \sum_{i=1}(N_i[I]\{U\}_i)$$

2. The stresses can be determined as

$$\{\sigma\} = [D](\{\epsilon\} - \{\epsilon_0\}) + \{\sigma_0\}$$

3. The loads are related to displacements with stiffness transformation

$$\{F\}^e = \left(\int_{vol} [B]^T[D][B]dv\right)\{U\}^e - \int_{vol}[B]^T[D]\{\epsilon_0\}dv + \int_{vol}[B]^T\{\sigma_0\}dv$$
$$- \int_s [N]^T\{F\}ds - \int_{vol}[N]^T\{\sigma\}dv$$
$$= [K]^e\{U\}^e + \{F_b\}^e + \{F_s\}^e + \{F_{\sigma 0}\}^e + \{F_{\epsilon 0}\}^e$$

where

$\{F_b\}$ body force, $\{F_{\sigma 0}\}$ force due to initial stresses

$\{F_s\}$ surface force, $\{F_{\epsilon 0}\}$ force due to initial strain

4. *Creep.*

Creep Burger model in pseudo-time, the incremental flow component and incremental delayed strain are algebraically added

$$\Delta J(t') = \Delta J_f(t') + \Delta J_\alpha(t')$$

where $\Delta J_f(t') = \Delta t'\rho(T) = [(t' + \Delta t') - t']\rho(T)$

$$\Delta J_\alpha(t') = [J_\alpha(t' + \Delta t') - J_\alpha(t')$$
$$= (1 - e^{-\beta\Delta t'})[Q - J_\alpha(t')]$$

$; Q = 14.21457 \times 10^{-6}\,\text{mm}^2/\text{N}$

$\beta = 0.2814 \times 10^6\,\text{N/mm}^2$

$t' =$ pseudo time

$\Delta t' =$ incremental pseudo time

$\rho(T) =$ temperature function

$J_f, J_\alpha =$ creep functions

Pseudo time is converted into real time

$$t' = [-15.37346 + 7.88977\log_e(t)] \times 10^{-6}$$

Creep strain, $\{\epsilon_t\} = \Delta J(t')[D]\{\sigma\}$

$$E(T) = E_{20}\left[1 - \frac{T - 20}{137}\right] \text{ for } 20° \leqslant T \leqslant 50°$$

$$E(T) = E_{20}(0.78)\left[1 - \frac{T - 50}{341}\right] \text{ for } 50° \leqslant T \leqslant 85°$$

APPENDIX II

CRACKING MATRICES

(1) Crack in Principal direction

'one'

$$D^*_{11} = D^*_{12} = D^*_{13} = D^*_{21} = D^*_{31} = 0$$

$$D^*_{22} = D_{22} - D_{12}D_{12}/D_{11}$$

$$D^*_{33} = D_{33} - D_{13}D_{13}/D_{11}$$

$$D^*_{23} = D_{23} - D_{12}D_{13}/D_{11}$$

$$D^*_{44} = a'D_{44}$$

$$D^*_{55} = D_{55}$$

$$D^*_{66} = a'D_{66}$$

(2) Crack in Principal direction 'Two'

$$D^*_{22} = D^*_{12} = D^*_{21} = D^*_{23} = D^*_{32} = 0$$

$$D^*_{11} = D_{11} - D_{21}D_{21}/D_{22}$$

$$D^*_{33} = D_{33} - D_{23}D_{23}/D_{22}$$

$$D^*_{13} = D_{13} - D_{12}D_{23}/D_{22}$$

$$D^*_{31} = D^*_{13}$$

$$D^*_{44} = a'D_{44}$$

$$D^*_{55} = a'D_{55}$$

$$D^*_{66} = D_{66}$$

(3) Crack in Principal direction 'Three'

$$D^*_{33} = D^*_{13} = D^*_{31} = D^*_{23} = D^*_{31} = 0$$

$$D^*_{11} = D_{11} - D_{13}D_{13}/D_{33}$$

$$D^*_{22} = D_{22} - D_{23}D_{23}/D_{33}$$

$$D^*_{12} = D_{12} - D_{13}D_{23}/D_{33}$$

$$D^*_{21} = D^*_{12}$$

$$D^*_{44} = D_{44}$$

$$D^*_{55} = a'D_{55}$$

$$D^*_{66} = a'D_{66}$$

(4) Crack in Principal direction 'one' and 'two'

$$D^*_{11} = D^*_{22} = D^*_{12} = D^*_{21} = 0$$

$$D^*_{13} = D^*_{31} = D^*_{23} = D^*_{32} = 0$$

$$D^*_{33} = D_{33} - D_{13}D_{13}/D_{11} - D_{23}D_{23}/D_{22}$$

$$D^*_{44} = a'D_{44}$$

$$D^*_{55} = a'D_{55}$$

$$D^*_{66} = a'D_{66}$$

(5) Cracks in Principal directions 'two' and 'three'

$$D^*_{22} = D^*_{33} = D^*_{23} = D^*_{32} = 0$$

$$D^*_{13} = D^*_{31} = D^*_{12} = D^*_{21} = 0$$

$$D^*_{11} = D_{11} - D_{21}D_{21}/D_{22} - D_{13}D_{13}/D_{23}$$

$$D^*_{44} = a'D_{44}$$

$$D^*_{55} = a'D_{55}$$

$$D^*_{66} = a'D_{66}$$

(6) Cracks in Principal directions 'three' and 'one'

$$D^*_{11} = D_{33} = D^*_{12} = D^*_{21} = 0$$

$$D^*_{13} = D^*_{31} = D^*_{23} = D^*_{31} = 0$$

$$D^*_{22} = D_{22} - D_{12}D_{12}/D_{11} - D_{23}D_{23}/D_{33}$$

$$D^*_{44} = a'D_{44}$$

$$D^*_{55} = a'D_{55}$$

$$D^*_{66} = a'D_{66}$$

where a' includes the influence of concrete aggregate interlocking.

(7) Cracks in all three Principal directions

$$[D^*] = [0]$$

دراسة تحليلية للشقوق الغير طولية ذات الأبعاد الثلاثة لأوعية التخزين الخرسانية سابقة الإجهاد

يعقوب فهد العبيد
كلية الدراسات التكنولوجية
الهيئة العامة للتعليم التطبيقي والتدريب
ص. ب: ٤٢٣٢٥ الشويخ ٧٠٦٥٤ الكويت

خلاصة

تزودنا هذه الدراسة بالتطور الكامل لشقوق الخرسانة الغير طولية ذات الأبعاد الثلاثة المستخدمة في الأوعية الإحتوائية.

ويشمل التحليل خلطة الصلب العادي، البطانة الفولاذية، أوتار الشد الخرسانية سابقة الاجهاد، وروابط الشد الخرسانية المتباينة الخواص وتماسك الخرسانة.

وتتناول الدراسة تحليل الشقوق من خلال برنامج الحاسب الآلي *OBAID* ثم مقارنة نتائج التحليل مع النتائج التي تم الحصول عليها من نموذج العينة.